Closure to "Minimum Specific Energy and Transcritical Flow in Unsteady Open-Channel Flow" by Oscar Castro-Orgaz and Hubert Chanson

DOI: 10.1061/(ASCE)IR.1943-4774.0000926

Oscar Castro-Orgaz[1] and Hubert Chanson[2]

[1]Professor of Hydraulic Engineering, Univ. of Cordoba, Campus Rabanales, Leonardo Da Vinci Bldg., E-14071 Cordoba, Spain (corresponding author). E-mail: ag2caoro@uco.es

[2]Professor in Hydraulic Engineering, School of Civil Engineering, Univ. of Queensland, Brisbane, QLD 4072, Australia. E-mail: h.chanson@uq.edu.au

The writers thank the discussers for their interest in the original paper, and the comments offered. During the inspection of the discussers' assertions, it was found that most of them were unsupported by hydraulic analysis. Detailed replies to each comment are given, with bullet points used to differentiate between specific items to be presented.

General

- First, it is clarified here that, contrary to the discussers' opening statements, the original paper explored the validity of the steady backwater equation, or gradually varied flow equation, at the critical depth. The validity of the equation was checked using an unsteady mathematical model, namely the Saint Venant equations, as well as through the experiments. The backwater equation is obtained by simplifying the differential form of Saint Venant equations to steady-state conditions (Montes 1998), namely

$$\frac{dh}{dx} = \frac{-\frac{dz_b}{dx}(x)}{1-\frac{q^2}{gh^3(x)}} = \frac{-\frac{dz_b}{dx}}{1-\mathrm{F}^2} \tag{1}$$

  where h = flow depth; q = discharge; and $z_b = z_b(x)$ = bottom profile. Comparison of the solution the backwater equation with the solution of the integral form of Saint Venant equations, after establishment of a steady state, gave identical results (Fig. 3 of the original paper). Comparison of Saint Venant equations with experimental data in Fig. 5(b) of the original paper gave good results. The analytical solution for the free surface slope at the critical point is

$$\left(\frac{dh}{dx}\right)_c = \pm\left(-\frac{h_c}{3}\frac{\partial^2 z_b}{\partial x^2}\right)^{1/2} \tag{2}$$

  This equation was compared and verified with the experiments of Wilkinson (1974) in Fig. 4 of the original paper. Using the unsteady-flow results from Saint Venant equations, the free surface slope at a section was computed from the finite-difference approximation

$$\frac{\partial h}{\partial x}(x,t) \approx \frac{h_{i+1}(t) - h_{i-1}(t)}{2\Delta x} \tag{3}$$

  At the weir crest ($x = 0$), it was found that the steady-state free surface slope obtained from the unsteady solution of Saint-Venant equation perfectly matched Eq. (2), e.g.,

$$\left.\frac{\partial h}{\partial x}(0,t)\right|_{t\to\infty} \to -\left[-\frac{1}{3}\left(\frac{q^2}{g}\right)^{1/3}\frac{\partial^2 z_b}{\partial x^2}\right]^{1/2}_{\text{crest}} \tag{4}$$

  This result was also included in Fig. 4 of the original paper. Therefore, the validity of the steady-state equations (backwater equation and singular point equation) was verified in the original paper, using both general unsteady mathematical solutions, and laboratory observations. To clearly highlight this fact, the computed free-surface profile using Eq. (1), obtained from the Runge-Kutta method, is presented in Fig. 1(a) [Fig. 5(b) of the original paper]. The boundary condition at the weir crest section, $x = 0$, is $h(0) = h_c = (q^2/g)^{1/3}$. The free surface slope at that section is given by Eq. (2). Subcritical and supercritical profiles were computed from $x = 0$ in the upstream and downstream directions, respectively. Fig. 1(a) reveals that the accuracy of the computation is good. That the Saint Venant theory is mathematically valid at the critical depth means that for the weir flow case investigated in the original paper, mathematical solutions are obtained for arbitrary values of $E_{\min}/R$. Consequently, limits to the theory should be set based on experimental observations. This was accomplished in the original paper on the basis of the computation presented in Fig. 5(b) [current Fig. 1(a)]. The mathematical prediction based on the backwater equation is good if the curvature is small, as in Fig. 1(a), where $E_{\min}/R = 0.253$. The experimental verification of Eq. (2) is presented in the current Fig. 1(b), based on Fig. 4 of the original paper. This analytical solution is seen to be in excellent agreement with experiments up to $-h_c d^2 z_b(x)/dx^2 \approx 0.15$, or $E_{\min}/R \approx 3/2 \cdot 0.15 = 0.225$. Therefore, the solution of the backwater Eq. (1), including Eq. (2), are in full agreement with the more general solution of Saint Venant equations, and these solutions are verified to be physically good if the curvature is small, e.g., for $E_{\min}/R < 0.25$.
- For steady, frictionless flow over a weir, Eq. (1) is equivalent to the differential form of

$$H = z_b + h + \frac{q^2}{2gh^2} = \text{const} \tag{5}$$

  It means that, based on Eq. (5), smooth mathematical solutions for transcritical flow over a weir are obtained [Fig. 1(a)]. Eq. (1) is consistent with the formation of steady singular points, asymptotically, during an unsteady flow computation based on the Saint Venant equations

$$\frac{\partial \mathbf{U}}{\partial t} + \frac{\partial \mathbf{F}}{\partial x} = \mathbf{S} \tag{6}$$

  where $\mathbf{U}$ = vector of conserved variables; $\mathbf{F}$ = flux vector; and $\mathbf{S}$ = source term vector, given by

$$\mathbf{U} = \begin{pmatrix} h \\ hU \end{pmatrix}; \qquad \mathbf{F} = \begin{pmatrix} hU \\ hU^2 + \frac{1}{2}gh^2 \end{pmatrix};$$
$$\mathbf{S} = \begin{bmatrix} 0 \\ gh(-\frac{\partial z_b}{\partial x} - S_f) \end{bmatrix} \tag{7}$$

  where U = depth-averaged velocity. Results in Figs. 3 and 4 of the original paper indicated that both results almost perfectly match, thereby indicating that the unsteady flow over a weir produces a singular point asymptotically in the crest section as the steady state is approached.

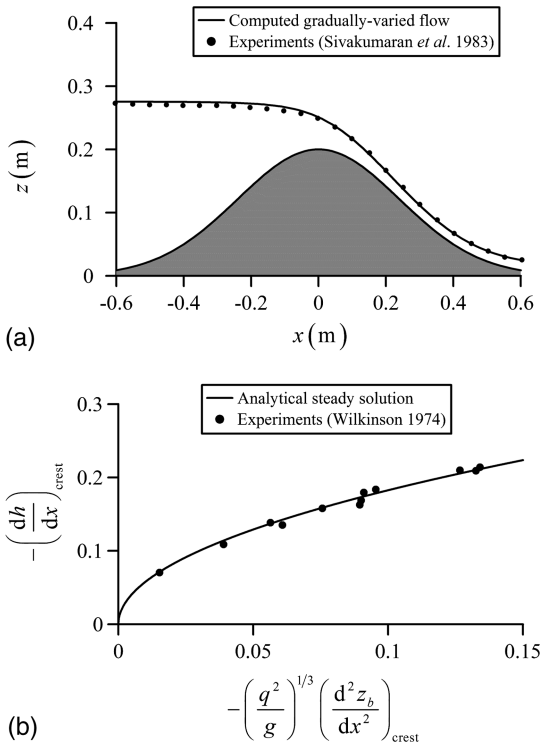

Fig. 1. (a) Free-surface profile computed applying the singular point method to the backwater equation, for a test case of Sivakumaran et al. (1983) with $E_{min}/R = 0.253$ and $q = 0.0359$ m^2/s; (b) experimental verification of the free-surface slope at a control section computed using the singular point method

- The discussers used the terminology Singular Point Theory, which is not adequate as such a theory does not exist, but rather the Singular Point Method, the term used by the writers in the original paper and by Chow (1959, pp. 237–242), among others. The singular point method is a mathematical technique used to solve indeterminations in ordinary differential equations. Therefore, it is a mathematical method that can be applied to different theories. It is a very common tool in applied mathematics (e.g., von Kármán and Biot 1940) used to model dynamic systems in physics and engineering.
- The normal depth concept is not used in the original paper, given that flow over a weir crest can be considered a potential flow, as verified experimentally (Montes 1998).
- Broad-crested weirs are not considered in the original paper, contrary to what the discussers suggested. The writers considered flow over a weir crest, where $z_b(x)$, $dz_b(x)/dx$ and $d^2z_b(x)/dx^2$ are smooth and continuous.
- In their experimental setup (Fig. 1 of in the discussion), the discussers found various singular points. To determine the actual flow profile, subcritical and supercritical profiles are computed from each singular point. Between each pair of singular points, a supercritical flow profile computed from the singular point upstream must be part of an ensemble with a subcritical flow profile computed from the singular point downstream, studying the formation of a hydraulic jump. If a jump is formed, both singular points acts as controls. If a jump is not formed, only one singular point will be an active control section, and the profile between the two singular points will be fully subcritical or supercritical. A characteristic feature of a singular point is the possibility of transcritical flow profiles across them, when it acts as a control, and the variety of profiles in its vicinity, not crossing it. The number of possible cases is long, and there is no space for a detailed description in this closure, but interested readers are referred to the work of Iwasa (1958).

Hydrostatic Modeling

- The discussers assert that "there is no reason for both numerator and denominator, each different functions of x and h, going to zero at the same point in (x, h) space," with reference to the singular point of Eq. (1). Mathematical proof is given as follows. Let Eq. (1) be written in the alternative form

$$\frac{dz_b}{dx} + \frac{dh}{dx}\left(1 - \frac{q^2}{gh^3}\right) = 0 \tag{8}$$

Define the function I of (x, h) space as

$$I(x,h) = \frac{dz_b}{dx} + \frac{dh}{dx}(1 - \mathsf{F}^2) \tag{9}$$

Any point of the (x, h) space that produces the following identity:

$$I(x,h) \equiv 0 \tag{10}$$

is by definition a solution of the ordinary differential equation (ODE) given by Eq. (8). Now, consider a point $x = x_o$ where $dz_b(x)/dx = 0$. Solutions of the ODE at this point must verify, therefore, the identity

$$I(x_o,h) = \frac{dh}{dx}(1 - \mathsf{F}^2) \equiv 0 \tag{11}$$

Based on Eq. (11), the following solutions (S_1, S_2, S_3) are possible at $x = x_o$:

$$\begin{aligned} &\frac{dh}{dx} = 0, \quad \mathsf{F} \neq 1 \rightarrow S_1 \\ &\frac{dh}{dx} \neq 0, \quad \mathsf{F} = 1 \rightarrow S_2 \\ &\frac{dh}{dx} = 0, \quad \mathsf{F} = 1 \rightarrow S_3 \end{aligned} \tag{12}$$

The three solutions given in Eq. (12) are mathematically possible, but the physical implication of each one is unclear. To depict physically what each mathematical statement in Eq. (12) indicates, Eq. (8) is differentiated with respect to x to get

$$\frac{d^2z_b}{dx^2} + \frac{d^2h}{dx^2}\left(1 - \frac{q^2}{gh^3}\right) + \left(\frac{dh}{dx}\right)^2 \frac{3q^2}{gh^4} = 0 \tag{13}$$

There is nothing assumed to get Eq. (13), as only a differential of Eq. (8) was determined. Now, conditions given by each solution (S_1, S_2, S_3) in Eq. (12) are complemented with the application of Eq. (13) to yield

$$\begin{aligned} &S_1 \Rightarrow \frac{dh}{dx} = 0, \quad \mathsf{F} \neq 1, \quad \frac{d^2z_b}{dx^2} + \frac{d^2h}{dx^2}\left(1 - \frac{q^2}{gh^3}\right) = 0 \\ &S_2 \Rightarrow \frac{dh}{dx} \neq 0, \quad \mathsf{F} = 1, \quad \frac{d^2z_b}{dx^2} + \left(\frac{dh}{dx}\right)^2 \frac{3q^2}{gh^4} = 0 \\ &S_3 \Rightarrow \frac{dh}{dx} = 0, \quad \mathsf{F} = 1, \quad \frac{d^2z_b}{dx^2} = 0 \end{aligned} \tag{14}$$

Based on the mathematical results in Eq. (14) the following points can be made:

1. Solution S_1 implies a subcritical ($\mathsf{F} < 1$), or supercritical ($\mathsf{F} > 1$), flow at the weir crest $[dz_b(x)/dx = 0]$, with zero free-surface slope. This is the well-known case of a whole subcritical, or supercritical profile, over a hump (e.g., Jain 2001, p. 98);
2. Solution S_2 implies a critical flow ($\mathsf{F} = 1$) at the weir crest $[dz_b(x)/dx = 0]$, with the free-surface slope given by Eq. (2). To get a physical solution, the condition $d^2z_b(x)/dx^2 < 0$ is required, that is, a critical flow section is formed only in weir flow (convex bottom profile) (e.g., Chanson 2006); and
3. Solution S_3 implies a critical flow ($\mathsf{F} = 1$) with $dz_b(x)/dx = 0$ and $d^2z_b(x)/dx^2 = 0$. This is the theoretical case of critical, frictionless flow over a horizontal bottom.

The present development is a generalization of a mathematical development by Henderson (1966, pp. 40–42). Solution S_2 is a general mathematical solution of Eq. (8), and, thus of Eq. (1). Therefore, there is not fortuitous occurrence of $dz_b(x)/dx = 0$ and $\mathsf{F} = 1$. The critical depth, with finite free-surface slope, is one of the possible solutions of the backwater equation. Inclusion of the friction slope is simple (e.g., Hager 2010, pp. 142–149), and it is not repeated here.

- Shock capturing finite-volume schemes using the Godunov upwind method, assisted by robust Riemann solvers, as used in the original paper, yields accurate solutions of shallow-water flows (Toro 2001). The integral form of Eq. (6) over a control volume is (Toro 2001)

$$\int_\Omega \frac{\partial \mathbf{U}}{\partial t} d\Omega + \int_A \mathbf{n} \cdot \mathbf{F} dA = \int_\Omega \mathbf{S} d\Omega \tag{15}$$

where Ω = control volume; A = cell boundary area; and $\mathbf{n}$ = outward unit vector normal to A. Eq. (15) was solved in the original paper using a high-resolution finite-volume scheme, where details of the numerical scheme were extensively described. An important aspect that should be clearly understood is that that the integral Eq. (15) is able to describe both continuous and discontinuous solutions for $\mathbf{U}(x, t)$, without any specific treatment as the flow crosses the critical depth. In the weir flow simulations presented in the original paper, the smooth solution at the weir crest was a mathematical result, found to be in perfect agreement with the singular point method applied to Eq. (1). In weir flow, steady transcritical solutions from $\mathsf{F} < 1$ to $\mathsf{F} > 1$ with $dh/dx \to \infty$ are not possible. However, these are possible in unsteady flow during the propagation of a shock wave (Fig. 6 of the original paper). In contrast, steady transcritical solutions from $\mathsf{F} > 1$ to $\mathsf{F} < 1$ with $dh/dx \to \infty$ are possible in the form of a hydraulic jump. All these cases of transcritical flow can be obtained from Eq. (15) without any specific treatment near the critical depth by using a high-resolution Godunov-type numerical scheme.

- The discussers asserted that "to describe general problems of transitional flow it is necessary to use, at least, Boussinesq equations." The Saint Venant equations provide very accurate solutions for some transitional flows. To demonstrate that two extreme transcritical test cases, widely used in open channel flows, were selected (e.g., Khan and Lai 2014, pp. 65–69). In Fig. 2, a dam break wave in a dry, rectangular, horizontal flume is considered. The flume is 0.093 m wide, 0.08 m in tall, and 20 m long. The dam was located at coordinate $x = 10$ m, and the removal was considered instantaneous. The tailwater portion of the flume was initially dry, and the water depth in the dam 0.074 m. Experimental measurements conducted

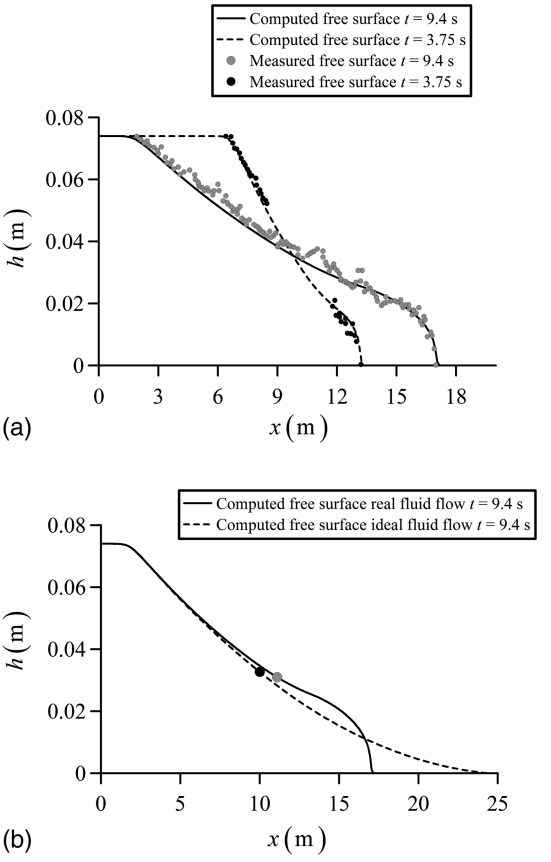

Fig. 2. Validity of Saint Venant equations for transcritical flow in a dry-bed dam break wave: (a) comparison of computed and measured instantaneous free-surface profiles (data from Schoklitsch 1917); (b) comparison of ideal and real fluid flow solutions at $t = 9.4$ s, and position of critical points (black circle and gray circle); computations using $\Delta x = 0.1$ m and CFL = 0.9

by Schoklitsch (1917) two times after removal of the dam, namely $t = 3.75$ s and $t = 9.4$ s, are plotted in Fig. 2(a). The flow was modeled using Eq. (15) and the numerical scheme of the original paper, introducing the dry bed case Riemann solver, and Manning's equation with $n = 0.009$ sm$^{-1/3}$ (Khan and Lai 2014). The effect of the friction slope was introduced implicitly in the numerical model to increase stability near the wet-dry front. A positivity preserving computational algorithm was used for the wet-dry front treatment (Khan and Lai 2014). As demonstrated in Fig. 2(a), Saint Venant equations can model transcritical open-channel flow with great accuracy. In Fig. 2(b), it is plotted the computed free-surface profile at $t = 9.4$ s, with indication of the position of the critical flow section, where $\mathsf{F} = U/(gh)^{1/2} = 1$. It can be observed that it is not located at the dam axis. Computations for ideal fluid flow ($S_f = 0$) yields a result identical to the parabolic, analytical solution by Ritter (Montes 1998; Chanson 2009)

$$x = x_{\text{dam}} + t[-3(gh)^{1/2} + 2(gh_o)^{1/2}] \tag{16}$$

where h_o = upstream water depth (= 0.074 m); and the dam coordinate $x_{\text{dam}} = 10$ m. For Ritter's solution, the flow is exactly critical at the dam axis (e.g., Jain 2001, p. 215). Therefore, the displacement of the critical point due to friction is seen to be small, and the main effect is confined to the shape of the front.

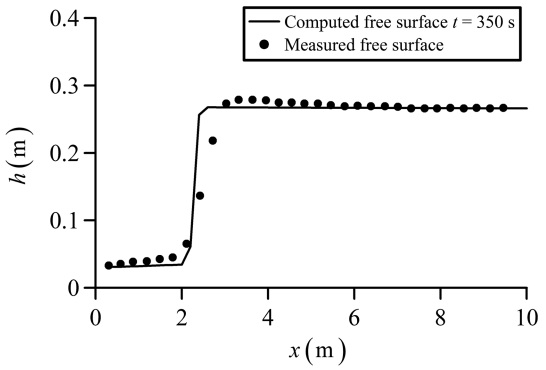

Fig. 3. Validity of Saint Venant equations for transcritical flow in a hydraulic jump; comparison of computed and measured steady free-surface profiles; computations using $\Delta x = 0.2$ m and CFL = 0.9 (data from Gharangik and Chaudhry 1991)

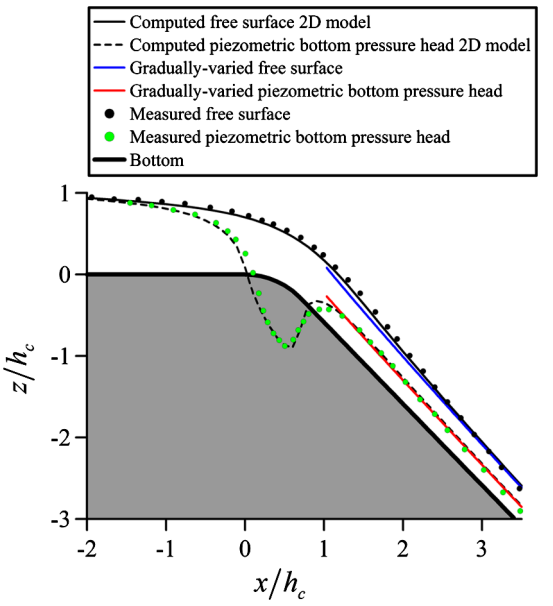

Fig. 4. Slope break problem with 45° chute slope; comparison of 2D potential flow solution, experimental data (data from Hasumi 1931), and 1D, potential, gradually varied flow solution

Resorting to Boussinesq equations in this case is therefore not needed.

A second test of Saint Venant equations for transcritical flow is presented in Fig. 3, where a hydraulic jump measured by Gharangik and Chaudhry (1991) is included. The channel is 14 m long, horizontal, and 0.46 m wide. The Manning's roughness coefficient is $n = 0.008$ s m$^{-1/3}$ (Khan and Lai 2014). The upstream boundary conditions for the supercritical flow are a water depth of 0.031 m, with a discharge of 0.118 m^2/s. At the downstream, subcritical section, only one boundary condition is set, namely the experimentally measured water depth of 0.265 m. The initial free-surface profile in the numerical model was taken as a static water layer of 0.031 m. The tailwater level was gradually increased from 0.031 to 0.265 m in 50 s in the numerical model. Computational results obtained at $t = 350$ s, once a steady state was reached, are displayed in Fig. 3. It can be seen that Saint Venant equations produce a good transcritical flow simulation, and resorting to Boussinesq equations in this test case is not needed.

Nonhydrostatic Modeling

- The discussers' Fig. 1 presented an experiment for flow over a broad-crested weir with a downstream chute slope of 45°, and an unexplained, undocumented, theoretical simulation. The lack of any detail in the discussion stating what equation was solved, and the fact that reference was made to unpublished results, made it impossible to elaborate a comment on this test and the discussers' theoretical results. They made reference to a "finite slope" Boussinesq theory, which could not be precisely understood by the writers. They also made reference to the Boussinesq theory by Matthew (1991), used by Castro-Orgaz and Hager (2009). A detailed reply to explain Boussinesq theory for flows where the bottom slope is finite will be given later.
- Resort to the problem of flows from a horizontal to a steep slope is made. Fig. 4 considers one test by Hasumi (1931) for a slope transition composed by a horizontal reach followed by a circular-shaped transition profile of $R = 0.1$ m that finishes in a steep slope reach of 45° inclination. This is similar to the discussers' experimental setup, therefore. The discharge is 0.987 m^2/s ($h_c = 0.10$ m). The measured free surface and piezometric bottom pressure head are plotted in the figure. The flow in open channel transitions, including a slope break, can be approximately modeled with the equations of an inviscid and irrotational flow (Montes 1998). The flow problem presented in Fig. 4 was modeled using the Laplacian for z as a function of the pair of variables (ψ, x)

$$\frac{\partial^2 z}{\partial x^2}\left(\frac{\partial z}{\partial \psi}\right)^2 + \frac{\partial^2 z}{\partial \psi^2}\left[1 + \left(\frac{\partial z}{\partial x}\right)^2\right] - 2\frac{\partial^2 z}{\partial x \partial \psi}\frac{\partial z}{\partial x}\frac{\partial z}{\partial \psi} = 0 \quad (17)$$

where ψ = stream function. The numerical model developed by Montes (1994) was applied, and is not further described here. The upstream and downstream boundary sections were located at $x/h_c = \pm 3$. Twenty streamlines were used to model this flow, and the energy level on the horizontal reach was set to $H/h_c = 1.5$. The two-dimensional (2D) computational results displayed in Fig. 4 show that the ideal fluid flow computation in the slope break problem produces good results. The potential flow approximation is shown, therefore, to be an acceptable approximation.
- To avoid the solution of the full 2D problem, as described earlier, approximate one-dimensional (1D) models for potential flow are desirable. Matthew (1991) developed an approximate Boussinesq theory, where the extended energy equation reads

$$H = z_b + h + \frac{q^2}{2gh^2}\left(1 + \frac{2hh_{xx} - h_x^2}{3} + hz_{bxx} + z_{bx}^2\right) = \text{const} \quad (18)$$

Here $h_x = dh/dx$; $h_{xx} = d^2h/dx^2$; $z_{bx} = dz_b/dx$; and $z_{bxx} = d^2z_b/dx^2$. The bottom pressure head of Matthew's theory is (Castro-Orgaz and Hager 2009)

$$\frac{p_b}{\gamma} = h + \frac{q^2}{2gh^2}(2hz_{bxx} + hh_{xx} - h_x^2 - 2z_{bx}h_x) \quad (19)$$

Based on Eqs. (18) and (19), the following observations are made: (1) the theory considers the effect of the curvature of the free surface and bottom, accounted for by the inclusion of $h_{xx} = d^2h/dx^2$ and $z_{bxx} = d^2z_b/dx^2$; and (2) the theory considers the effect of the slope of the free surface and bottom, accounted for by the inclusion of $h_x = dh/dx$ and $z_{bx} = dz_b/dx$. The values

of these slopes and curvatures are not necessarily small ones. Therefore, Matthew's (1991) theory, used by Castro-Orgaz and Hager (2009), is an approximate potential flow model that includes the effects of finite curvatures and slopes. Friction is not included, however. This limits the application of Matthew's theory to a computational domain where the energy slope can be taken horizontally, as done by Montes (1994) and Castro-Orgaz and Hager (2009). Results of Castro-Orgaz and Hager (2009) solving Eq. (18) were in good agreement with Eq. (17), and with experimental observations.

- Castro-Orgaz and Hager (2009) analyzed the limits of the singular point method, applied to the backwater equation, for a slope break. They applied this method to Eq. (1) for slope breaks involving highly curved flows, and concluded that a model based on Eq. (1) cannot be applied where the curvature is strong, e.g., in the vicinity of the slope break. This is in full agreement with the original paper, where it was demonstrated that the singular point method applied to Eq. (1) produces good results where the curvature is weak, e.g., see Fig. 1(a). Both works are, therefore, in full agreement.
- Castro-Orgaz and Hager (2009) found that, despite Eq. (1) cannot be applied at the crest zone given the highly curved flow, it is a good approximation in the downstream slope for $x/h_c > 1$. For illustrative purposes, consider flows away from the crest, where streamline curvature effects can be neglected. The flow is gradually varied, meaning that the variation of h with x is small (this hypothesis is confirmed by the experimental results plotted in Fig. 4). For these flows, it can be assumed that $h_x^2 \approx h_{xx} \approx 0$. Furthermore, on the slope, the bed is flat, resulting $z_{bxx} = 0$. On this slope, however, the term z_{bx} is finite and equal to unity in this case. Therefore, despite h_x being small, the product $(h_x \cdot z_{bx})$ remains finite. Therefore, Eqs. (18) and (19) for gradually-varied, 1D potential flow on a finite slope read as follows:

$$H = z_b + h + \frac{q^2}{2gh^2}(1 + z_{bx}^2) \tag{20}$$

$$\frac{p_b}{\gamma} = h - \frac{q^2}{2gh^2}(2z_{bx}h_x) \tag{21}$$

Castro-Orgaz and Hager (2009) differentiated Eq. (20), producing for large F the ODE

$$\frac{dh}{dx} = \frac{z_{bx}}{\frac{q^2}{gh^3}(1 + z_{bx}^2)} \tag{22}$$

For the horizontal slope reach, the solution of Eq. (22) involving critical flow is solution S_3 in Eq. (12). Therefore, the theoretical flow profile is a horizontal line composed of an infinite number of critical points (Castro-Orgaz and Hager 2009). Taking as a boundary condition the critical point at the beginning of the slope break, the analytical solution of Eq. (22) for a finite slope is (Castro-Orgaz and Hager 2009)

$$\frac{h}{h_c} = \left(1 - \frac{2z_{bx}}{1 + z_{bx}^2}\frac{x}{h_c}\right)^{-1/2} \tag{23}$$

Inserting Eq. (22) into Eq. (21), the bottom pressure head is

$$\frac{p_b}{\gamma} = h - \frac{q^2}{2gh^2}(2z_{bx}h_x) = h\left(1 - \frac{z_{bx}^2}{1 + z_{bx}^2}\right) = \frac{h}{1 + z_{bx}^2} \tag{24}$$

Eq. (24) is the finite slope approximation for the bottom pressure head in gradually varied flows, to which the discussers made reference, quoting Fenton (2014, quoted in the discussion paper). Therefore, based on potential, gradually varied flow, finite slopes are accounted for both in free-surface and bottom-pressure-head computations. The results of the computations based upon Eqs. (23) and (24) are plotted in Fig. 4, for $x/h_c > 1$, as recommended by Castro-Orgaz and Hager (2009). It can be observed that the results are in excellent agreement with experiments and 2D numerical solution.

- If application of a Boussinesq model with friction is found to be necessary, resort to the development by Khan and Steffler (1996) can be made. The Boussinesq version of their theory, for steady flow, reads

$$\frac{d}{dx}\left(U^2 h + \frac{h}{2}\frac{p_b}{\rho}\right) = -\frac{p_b}{\rho}\frac{\partial z_b}{\partial x} - \frac{\tau_b}{\rho} \tag{25}$$

$$p_b = \rho g h + \rho\frac{U^2}{2}(hh_{xx} - h_x^2 - 2h_x z_{bx} + 2hz_{bxx}) + \tau_b\frac{\partial z_b}{\partial x} \tag{26}$$

where τ_b = bed shear stress. Eqs. (25) and (26) can be coupled to produce a simple ODE. Eq. (26) is a generalization of Eq. (19), where the effect of τ_b on p_b is accounted for.
- To show the general applicability of the singular point method, at the time that it is further demonstrated that Boussinesq equations are not the only model that can produce good transcritical flow simulations, consider Dressler (1978) theory for flow over curved beds. For steady flow, the theory gives the following ODE (Sivakumaran and Yevjevich 1987), after rearrangement:

$$\frac{dN}{d\xi} = \frac{-\sin\theta_b(1 - \kappa_b N) - \frac{q^2}{g}\kappa_b\frac{d\kappa_b}{d\xi}\frac{\ln(1-\kappa_b N)+\kappa_b N}{[(1-\kappa_b N)\ln(1-\kappa_b N)]^3}}{\cos\theta_b + \frac{q^2}{g}\kappa_b^3\frac{\ln(1-\kappa_b N)+1}{[(1-\kappa_b N)\ln(1-\kappa_b N)]^3}} = \frac{\Phi_1(N,\xi)}{\Phi_2(N,\xi)} \tag{27}$$

where ξ = bottom-fitted coordinate; $\kappa_b = \kappa_b(\xi)$ = curvature of the bottom profile; θ_b = local inclination angle of the bottom profile, $z_b(\xi)$, with the horizontal plane; and N = distance from the channel bottom to the free surface, measured orthogonally outward from the bottom curve. Using the same mathematical development presented with Eqs. (8)–(14), it can be demonstrated that at a weir crest, the flow is critical, and Eq. (27) is indeterminate. Consider flow over a hump (Fig. 5) for a test case of Sivakumaran et al. (1983) with $E_{\min}/R = 0.516$ and $q = 0.11197$ m^2/s [test of Fig. 5(a) in the original paper]. The critical depth for Dressler's theory is computed setting to zero the denominator of Eq. (27) (Dressler 1978)

$$\Phi_2(N_c,\xi) = \cos\theta_b + \frac{q^2}{g}\kappa_b^3\frac{\ln(1-\kappa_b N_c)+1}{[(1-\kappa_b N_c)\ln(1-\kappa_b N_c)]^3} = 0 \tag{28}$$

The solution of the nonlinear Eq. (28) by the Newton-Raphson method gave the crest flow depth. Eq. (27) was then integrated using the Runge-Kutta method in the upstream and downstream directions, starting at the crest. After removal of the indetermination at the weir crest (c), the free surface slope at the crest was found to be

$$\left(\frac{dN}{d\xi}\right)_c = -\frac{\left(\frac{\partial\Phi_1}{\partial\xi}\right)_c^{1/2}}{\left(\frac{\partial\Phi_2}{\partial N}\right)_c^{1/2}} \tag{29}$$

where

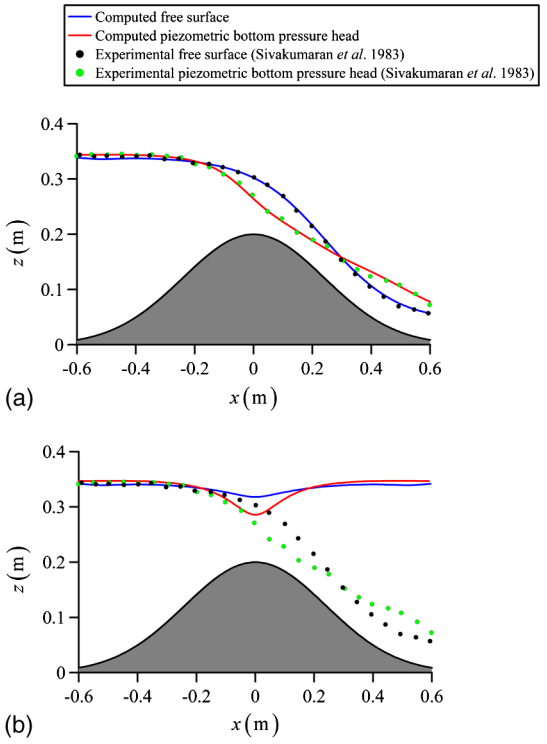

Fig. 5. Flow over a hump for a test case of Sivakumaran et al. (1983) with $E_{\min}/R = 0.516$ and $q = 0.11197$ m^2/s: (a) application of the singular point method to compute transcritical flow using Dressler theory; simulations are conducted without using any experimental measurement; (b) solution of Dressler theory based on the upstream experimental measurement

$$\left(\frac{\partial \Phi_1}{\partial \xi}\right)_c = -\kappa_b(1-\kappa_b N_c) \tag{30}$$

$$\left(\frac{\partial \Phi_2}{\partial N}\right)_c = 3\frac{q^2\kappa_b^4}{g}\frac{[\ln(1-\kappa_b N_c)+(5/6)]^2+(11/36)}{[(1-\kappa_b N_c)\ln(1-\kappa_b N_c)]^4} \tag{31}$$

Computational results are displayed in Fig. 5(a), showing good agreement with experimental measurements. The bottom pressure profile p_b was computed from (Dressler 1978)

$$p_b = \rho g N\cos\theta_b + \rho\frac{q^2\kappa_b^2}{2[\ln(1-\kappa_b N)]^2}\left[\frac{1}{(1-\kappa_b N)^2}-1\right] \tag{32}$$

showing again good agreement with observations in Fig. 5(a). These results demonstrate that the singular point method is a mathematical technique that can be applied to different theories, and that transcritical flow problems can also be tackled with other approximations different from Boussinesq equations. Eq. (27) was alternatively solved in Fig. 5(b) taking as starting point the experimentally measured water depth upstream of the hump. Computational results presented in Fig. 5(b) reveals that a subcritical flow profile along the entire hump is formed, as found by Sivakumaran et al. (1983). A supercritical flow profile can also be determined. This solution was forced by the upstream experimental water depth, which does not permit the flow to pass across the critical depth. A recent experimental verification of the singular point method was presented by Kabiri-Samani et al. (2014).

Concluding Remarks and Recommendation

- The singular point method is a useful tool to be used when needed. It has been experimentally verified. As to which model should be proposed to compute transcritical flows, common sense dictates the path to follow. Saint Venant equations are a good model in most cases, like for the computation of the flood-inundation area in river flows. If the computation of bed pressures is the main concern, then resort to Boussinesq equations can be made, e.g., for the determination of cavitation risk in a dam spillway crest. Between these two extremes are intermediate options, like use of Dressler theory.
- Since the pioneering work of Bélanger (1828), a number of scholars added to the general body of knowledge available today in the field of open channel hydraulics. It is suggested to modelers and researchers to keep in mind all these computational tools, including the singular point method, to continue advances in this fascinating field of research.

References

Bélanger, J. B. (1828). "On the numerical solution of some steady water flow problems (Essai sur la solution numérique de quelques problèmes relatifs au mouvement permanent des eaux courantes)." Carilian-Goeury, Paris (in French).

Castro-Orgaz, O., and Hager, W. H. (2009). "Curved streamline transitional flow from mild to steep slopes." *J. Hydraul. Res.*, 47(5), 574–584.

Chanson, H. (2006). "Minimum specific energy and critical flow conditions in open channels." *J. Irrig. Drain. Eng.*, 10.1061/(ASCE)0733-9437(2006)132:5(498), 498–502.

Chanson, H. (2009). "Application of the method of characteristics to the dam break wave problem." *J. Hydraul. Res.*, 47(1), 41–49.

Chow, V. T. (1959). *Open channel hydraulics*, McGraw-Hill, New York.

Dressler, R. F. (1978). "New nonlinear shallow flow equations with curvature." *J. Hydraul. Res.*, 16(3), 205–222.

Gharangik, A., and Chaudhry, M. (1991). "Numerical simulation of hydraulic jump." *J. Hydraul. Eng.*, 10.1061/(ASCE)0733-9429(1991)117:9(1195), 1195–1211.

Hager, W. H. (2010). *Wastewater hydraulics: Theory and practice*, Springer, Berlin.

Hasumi, M. (1931). "Untersuchungen über die Verteilung der hydrostatischen Drücke an Wehrkronen und -Rücken von Überfallwehren infolge des abstürzenden Wassers." *J. Dept. Agric. Kyushu Imperial Univ.*, 3(4), 1–97 (in German).

Henderson, F. M. (1966). *Open channel flow*, MacMillan, New York.

Iwasa, Y. (1958). "Hydraulic significance of transitional behaviours of flows in channel transitions and controls." *Mem. Facil. Eng., Kyoto Univ.*, 20(4), 237–276.

Jain, S. C. (2001). *Open channel flow*, Wiley, New York.

Kabiri-Samani, A., Rabei, M. H., Safavi, H., and Borghei, S. M. (2014). "Experimental-analytical investigation of super- to subcritical flow transition without a hydraulic jump." *J. Hydraul. Res.*, 52(1), 129–136.

Khan, A. A., and Lai, W. (2014). *Modelling shallow water flows using the discontinuous Galerkin method*, Taylor and Francis, London.

Khan, A. A., and Steffler, P. M. (1996). "Vertically averaged and moment equations model for flow over curved beds." *J. Hydraul. Eng.*, 10.1061/(ASCE)0733-9429(1996)122:1(3), 3–9.

Matthew, G. D. (1991). "Higher order one-dimensional equations of potential flow in open channels." *Proc. ICE*, 91(3), 187–201.

Montes, J. S. (1994). "Potential flow solution to the 2D transition from mild to steep slope." *J. Hydraul. Eng.*, 10.1061/(ASCE)0733-9429(1994)120:5(601), 601–621.

Montes, J. S. (1998). *Hydraulics of open channel flow*, ASCE, Reston VA.

Schoklitsch, A. (1917). "Über dambruchwellen." *Kaiserliche Akademie der Wissenschaften, Wien, Mathematisch-Naturwissenschaftliche Klasse, Sitzungberichte IIa*, 126, 1489–1514 (in German).

Sivakumaran, N. S., Tingsanchali, T., and Hosking, R. J. (1983). "Steady shallow flow over curved beds." *J. Fluid Mech.*, 128(1), 469–487.

Sivakumaran, N. S., and Yevjevich, V. (1987). "Experimental verification of the Dressler curved-flow equations." *J. Hydraul. Res.*, 25(3), 373–391.

Toro, E. F. (2001). *Shock-capturing methods for free-surface shallow flows*, Wiley, New York.

von Kármán, T., and Biot, M. A. (1940). *Mathematical methods in engineering: An introduction to mathematical treatment of engineering problems*, McGraw-Hill, New York.

Wilkinson, D. L. (1974). "Free surface slopes at controls in channel flow." *J. Hydraul. Div.*, 100(8), 1107–1117.